Virology 505 (2017) 181–192

Contents lists available at ScienceDirect

Virology

journal homepage: www.elsevier.com/locate/yviro

Tissue tropism of Saint Louis encephalitis virus: Histopathology triggered by epidemic and non-epidemic strains isolated in Argentina

María Elisa Rivarola[a,b,*], Guillermo Albrieu-Llinás[a,b], María Belén Pisano[a,b], Laura Beatriz Tauro[a,b], Melisa Gorosito-Serrán[b,c], Cristian Gabriel Beccaria[b,c], Luis Adrián Díaz[a,b], Ana Vázquez[b,d,e], Agustín Quaglia[a,b], Cristina López[b,f], Lorena Spinsanti[a,b], Adriana Gruppi[b,c], Marta Silvia Contigiani[a,b]

[a] *Laboratorio de Arbovirus, Instituto de Virología "Dr. J. M. Vanella", Facultad de Ciencias Médicas, Universidad Nacional de Córdoba, Enfermera Gordillo Gómez S/N. CP, 5016, Ciudad Universitaria, Córdoba, Argentina*
[b] *Instituto de Investigaciones Biológicas y Tecnológicas, CONICET-Universidad Nacional de Córdoba, Av. Velez Sarfield 1611, CP: 5016, Córdoba, Argentina*
[c] *Inmunología, Departamento de Bioquímica Clínica, Facultad de Ciencias Químicas, Universidad Nacional de Córdoba, Av. Medina Allende y Haya de la Torre. CP: 5016, Córdoba, Argentina*
[d] *Instituto de Salud Carlos III. Carretera de Majadahonda - Pozuelo, Km. 2.200. 28220 - Majadahonda (Madrid)*
[e] *CIBER de Epidemiología y Salud Pública (CIBERESP), Spain*
[f] *Instituto de Biología Celular. Facultad de Ciencias Médicas, Universidad Nacional de Córdoba, Juan Filloy S/N. PC: 5000, Ciudad Universitaria, Córdoba, Argentina*

ARTICLE INFO

Keywords:
Arbovirus
Saint Louis encephalitis virus
Tissue tropism
Histopathology
Pathogenesis

ABSTRACT

Saint Louis encephalitis virus (SLEV) reemerged in South America, and caused encephalitis outbreaks at the beginning of the 21st century. To enhance our knowledge about SLEV virulence, we performed comparative pathogenesis studies in Swiss albino mice inoculated with two different variants, the epidemic strain CbaAr-4005 and the non-epidemic strain CorAn-9275. Only the infection of mice with SLEV strain CbaAr-4005 resulted in high viremia, invasion of peripheral tissues including the lungs, kidney, and spleen, and viral neuroinvasion. This was associated with inflammatory pathology in the lungs, spleen, and brain as well as morbidity and mortality. In contrast, neither signs of desease nor viral replication were observed in mice infected with strain CorAn-9275. Interestingly, important loss of B cells and development of altered germinal centers (GC) were detected in the spleen of mice infected with strain CbaAr-4005, whereas mice infected with SLEV CorAn-9275 developed prominent GC with conserved follicular architecture, and neutralizing antibodies.

1. Introduction

Saint Louis encephalitis virus (SLEV, genus *Flavivirus*, family *Flaviviridae*) is a neurotropic flavivirus, endemic to the Americas. In South America, it is a reemerging arbovirosis with human cases reported in Argentina and Brazil (Spinsanti et al., 2003, 2008; Rocco et al., 2005; Mondini et al., 2007). SLEV reemerged in the central region of Argentina in 2002, after 17 years of no apparent epidemic activity (Spinsanti et al., 2003); since then, outbreaks were reported in the provinces of Córdoba (2005) (Spinsanti et al., 2008), Entre Ríos (2006), Buenos Aires (2010) and San Juan (2011) (Seijo et al., 2011).

The virus is maintained in a natural enzootic cycle between mosquitoes and birds (Reisen, 2003), although incidental infections are possible in humans and other mammals, which are typically dead-end hosts. According to published epidemiological data, human infections with SLEV are mostly asymptomatic or result in mild malaise of short duration, especially in young or middle-aged patients (Powell and Kappus, 1978; Reisen, 2003). Illness severity ranges from transient fever and headache to severe neurological disease, including meningitis and encephalitis and permanent neurological damage or even increased risk of death in the elderly (Calisher, 1994).

Across their geographic distribution, SLEV strains show genetic and

* Corresponding author at: Laboratorio de Arbovirus, Instituto de Virología "Dr. J. M. Vanella", Facultad de Ciencias Médicas, Universidad Nacional de Córdoba. Enfermera Gordillo Gómez S/N. CP: 5016. Ciudad Universitaria. Córdoba, Argentina.
E-mail addresses: mariaelisarivarola@gmail.com (M.E. Rivarola), guillermoalbrieu@gmail.com (G. Albrieu-Llinás), mbelenpisano@gmail.com (M.B. Pisano), lauratauro@gmail.com (L.B. Tauro), meli.s87@hotmail.com (M. Gorosito-Serrán), cristian.beccaria@gmail.com (C.G. Beccaria), ladriandiaz@gmail.com (L.A. Díaz), a.vazquez@isciii.es (A. Vázquez), quaglia.agu@gmail.com (A. Quaglia), cristinablopez@yahoo.com.ar (C. López), l_spinsanti@yahoo.com.ar (L. Spinsanti), agruppi@hotmail.com (A. Gruppi), martascontigia@hotmail.com (M.S. Contigiani).

http://dx.doi.org/10.1016/j.virol.2017.02.023
Received 22 March 2016; Received in revised form 7 February 2017; Accepted 28 February 2017

biological variation (Bowen et al., 1980; Kramer and Chandler, 2001; Rodrigues et al., 2010) and were classified as high, intermediate and low viremic/pathogenic strains (Bowen et al., 1980; Monath et al., 1980). In a previous study, we demonstrated in murine model that the high epidemic CbaAr-4005 strain was more infective and lethal than the other two non-epidemic strains (CorAn-9275 and 78V-6507) isolated in different epidemiological scenarios (Rivarola et al., 2014). Several studies have explored the pathogenicity of different neurotropic viruses in murine models (Weiner and Cole, 1970; Monath, 1980; Trent et al., 1980; Griffin et al., 1994; Kramer and Bernard, 2001; Diamond et al., 2003; Wang et al., 2003; Vogel et al., 2005; Brown et al., 2007; Steele and Twenhafel, 2010; Ong et al., 2014), but the question of how an epidemic SLEV causes disease in mice is still open.

In order to acquire a deeper understanding of SLEV pathogenesis, in the present study we performed comparative pathogenesis studies with different strains of SLEV, isolated under different epidemiological conditions, in terms of viremia kinetics, tropism, and histopathology in different visceral organs and brains of experimentally inoculated mice.

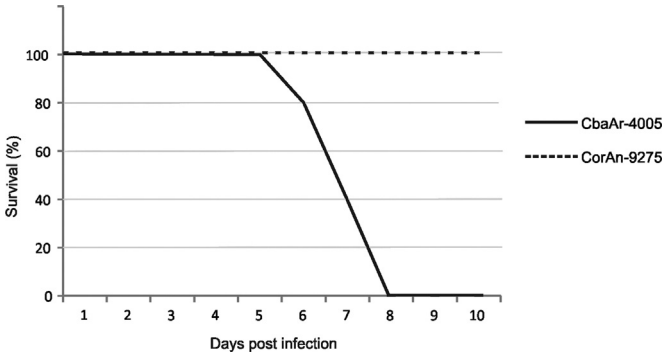

Fig. 2. Survival curves from R-W1 mice inoculated with CbaAr-4005 or CorAn-9275 SLEV strains. A group of 5 mice were inoculated with 3000–5000 PFU/mL of both viral strains by dorsal injection and followed for 15 days. The survival curves were constructed using data from three independent experiments. (Single column-fitting image).

2. Results

When R-W1 mice were infected with two different SLEV strains we observed that viremia was only detected in mice inoculated with the epidemic strain CbaAr-4005 (Fig. 1) between days 2 and 5 post-infection (p.i.), and reached the highest values between days 2 and 3 to finally decrease on day 5 p.i. Viremia was detectable neither in control mice nor in those mice infected with SLEV CorAn-9275 (data not shown). All the CbaAr-4005 infected mice showed evident signs of illness such as excitability, tremor, laterality on gait, and convulsion within days 6 and 7 p.i., and these symptoms were rapidly followed by death on day 8 p.i. (Fig. 2). In Fig. 2 we can observe that CbaAr-4005 infected mice start to die on day 6 p.i. and by day 8 p.i. all mice are dead. In contrast, clinical signs, viral load and mortality were observed neither in control mice nor in those mice infected with SLEV CorAn-9275. Seroconversion was evaluated in mice inoculated with both strains at days 4, 6, 8, 10 and 15 p.i., but specific antibodies (Abs) were only detected in mice infected with SLEV CorAn-9275 at day 15 p.i. Considering that mice infected with SLEV CbaAr-4005 did not survive more than 8 days p.i, it was not possible to evaluate the humoral response in them at days 10 and 15 p.i. (data not shown).

The evaluation of viral tropism using qRT-PCR showed dependence between organs and days p.i. ($F=615.59$, $p < 0.0001$, DF=32, pseudo-$R^2=0.9115128$) (Fig. 1). The spleen and kidneys of mice infected with the epidemic strain CbaAr-4005 showed low number of copies among days 1–4. In the spleen a low increase was registered on days 3, 5, 7, and a relatively higher raise was observed on day 8 p.i. ($p < 0.01$). In kidneys, a slight increase in the number of copies was observed during days 2 and 3 in comparison to days 1, 4, 5 and 6 p.i. ($p < 0.001$), and the viral load decreased significantly later on day 7 p.i. ($p < 0.001$), with no detection at all on day 8 p.i. No copies were detected in lung during the first four days of infection. The first detection was registered on day 5 p.i. ($p < 0.01$), and the load peak occurred only on day 6 p.i. ($p < 0.01$). Copy numbers rose substantially from 0 to 5203801 between days 4 and 5 p.i., and then increased significantly on day 6 p.i., to finally decrease during the last two days ($p < 0.001$). In brain, the viral load was detected when the viremia started to decrease, at 5 days p.i., increased at 6 days p.i. and it was still high at the moment of death. No viral particles were detected at all in the organs of mice infected with the non-epidemic strain CorAn-9275, which was in agreement with the absence of viremia. The specific amplification of the negative strand of SLEV RNA only showed positive results in the brain (days 5, 6, 7, and 8 p.i.) of mice infected with the epidemic strain, indicating that SLEV CbaAr4005 replicates in this organ (data not shown).

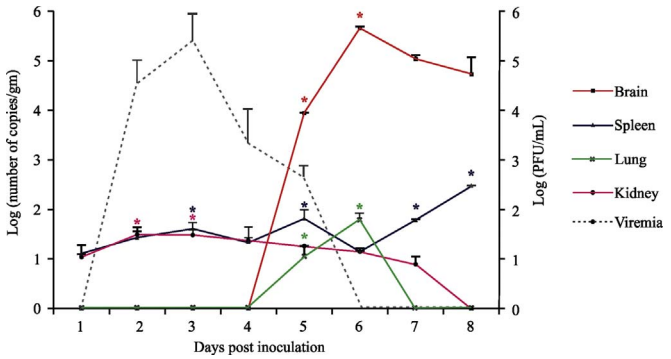

Fig. 1. Viremia and mean logarithm of the number of copies detected by qRT-PCR in organs of R-W1 mice inoculated with CbaAr-4005 strain. Viremia was recorded during 8 consecutive days after infection (dotted line), and the results were expressed as the log PFU/mL. For the number of copies detected in organs (color lines) the values were obtained by means of qRT-PCR. Data are expressed as log of number of copies. (*) Indicates statistically significant increases in the number of copies for each particular organ ($p < 0.05$). (1.5 column-fitting image).

Considering that there was a strong difference, in terms of infectivity, between both SLEV strains *in vivo*, we also compared the replication of CorAn-9275 and CbaAr-4005 strains in cell cultures. We observed that the viral growth curve in Vero and Raw 264.7 cells was significantly lower for SLEV CorAn-9275 than for CbaAr-4005 (Fig. 3), suggesting that the non-epidemic strain has a lower infection efficiency and/or restricted replication ability *in vitro*, in comparison to the epidemic strain.

Taking into account that the spleen is one of the target organs in which SLEV was detected (see Fig 1), and that it harbors cells from the immune system that are important for antiviral defense, we evaluated the splenic changes after infection by HE and immunostaining. In comparison to the structure of the spleen of control mice (Fig. 4a, b), by HE we observed that the spleens of infected mice with either viral strain showed important modifications in their architecture. Interestingly, in mice infected with CbaAr-4005 the follicles were small, highly diffused and showed an irregular structure. Inside the follicles, the germinal centers (GC) had low cellularity. The red pulp also presented areas with low cellularity and necrosis (Fig. 4c and e). The spleens of mice infected with CorAn-9275 were noticeably enlarged and they showed follicles with prominent and well organized GCs (Fig. 4d and f). The spleens of mice infected with both SLEV strains also had megakaryocytic hyperplasia (Fig. 4g and h).

By immunofluorescence, we observed a severe depletion of B cells in the spleens of mice infected with SLEV CbaAr-4005 compared to the control mice (Fig. 5a-b). SLEV CbaAr-4005 infected mice showed quite atrophic B lymphoid follicles, GCs markedly reduced in size and number and an atypical distribution of B cells surrounding periarteriolar lymphoid sheaths (Fig. 5c-d). On the contrary, the spleens of mice

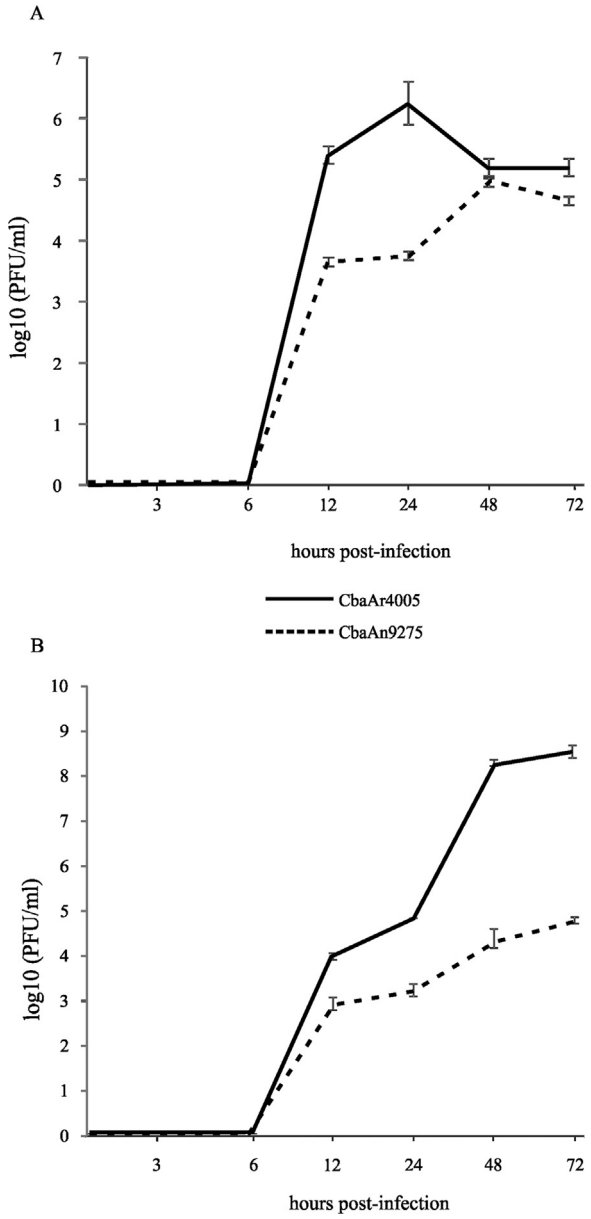

Fig. 3. In vitro replication curves of SLEV. Vero (a) and Raw 264.7 (b) cells infected with CbaAr-4005 (continuous line) and CorAn-9275 (dashed line) SLEV strains. The replication curves were constructed using data from three independent experiments.

infected with SLEV CorAn-9275 kept their follicular architecture, with many GCs developed inside the follicles (Fig. 5b).

Kidneys were apparently not affected by SLEV infection since they showed normal general appearance after infection with both virus strains (data not shown).

Compared to uninfected mice (Fig. 6a), the microscopic observation of lungs from CbaAr-4005 infected mice showed thickened alveolar septa (Fig. 6b) with inflammatory (lymphocytic) infiltrate expressed as interstitial pneumonia with collapsed alveolar sacs (Fig. 6c).

Histological analyses of the brain showed inflammatory infiltrate in the meninges (Fig. 7) and sporadic inflammatory infiltrate around blood vessels (Fig. 8). By HE staining in several regions we observed high densities of small pyknotic nuclei, with irregular membranes and apoptotic appearance (Fig. 9a-c). In order to examine the possible occurrence of apoptosis in brains of infected mice, we used TUNEL labeling to detect local DNA damage. The examination of sagittal sections of CbaAr-4005-infected brains revealed the presence of apoptotic cells (TUNEL+) in the cortex (Fig. 9e), whereas no fluorescent cells were detected in the brains of control mice (Fig. 9d).

3. Discussion

To enhance our knowledge about virulence of SLEV, we focused the present study on detailed analyses of viremia, viral tropism, and histopathology in different organs using a murine model which has been proved to be very useful for the study of different aspects of the flavivirus infection (Monath et al., 1980; Muylaert et al., 1996; Matthews et al., 2000; Brown et al., 2007; Barth et al., 2007; Rivarola et al., 2014).

Detectable viremia was only observed after infection with the epidemic strain CbaAr-4005. This result is consistent with findings reported by Monath et al. (1980) who observed that SLEV strains isolated in epidemic scenarios caused higher viremia levels in Swiss albino mice than strains isolated from regions with enzootic activity of SLEV. Moreover, recent evidence suggests that virulent/pathogenic phenotype in SLEV is associated with the biological source of viral isolation. Diaz et al. (2015) detected that viral strains isolated from mosquitoes, like CbaAr-4005, are likely to be more virulent and pathogenic than those isolated from mammals.

When we evaluated viral tropism using qRT-PCR, we only detected RNA copies in all the tested tissues from mice infected with CbaAr-4005. The lack of detection of virus in tissues and blood after the infection with CorAn-9275 strain could be due to several factors. One of them could be the different replication capacities between strains. When we evaluated the growth curve of the two SLEV strains in Vero and Raw 264.7 cells, we observed a significantly lower replication capacity of CorAn-9275, which is consistent with the milder virulence of this strain (Rivarola et al., 2014). Other factor could be the rapid elimination of viral particles by the host immune system (Monath and Borden, 1971; Ben-Nathan et al., 1996; Wang et al., 2003; Samuel and Diamond, 2006; King et al., 2007; Mehlhop and Diamond, 2007; Steele and Twenhafel, 2010). It has been proposed that amino acidic changes in coding and non-coding regions can affect the biological behavior (virulence, neuroinvasiveness and viremia profiles) and adaptive features of viruses (Muylaert et al., 1996; Pletnev et al., 1993; McMinn, 1997; Mandl et al., 2000; Arroyo et al., 2001; Beasley et al., 2004). Following this premise, Díaz et al. (2015) characterized the complete genome of epidemic and non-epidemics SLEV strains, including CbaAr-4005 and CorAn9275 strains, and found seventeen amino acid changes, ten of which were non-conservative and located in proteins E, NS1, NS3, and NS5. However, no statistically significant differences were observed between individual point mutations and their possible effect on differential phenotypes related to viremia and/or pathogenesis, although interactions among them should be considered in a deeper genomic analysis. In order to analyze the possible impact of mutational changes on the virus phenotype, future studies will require the development of a reverse genetics system.

Although replication in spleen was previously reported in mice infected with other neurotropic flaviviruses (Solomon and Vaughn, 2002; Diamond et al., 2003; Brown et al., 2007), based on our results we cannot confirm viral replication of SLEV in this organ, since no detectable PCR products were obtained by means of negative strand-specific amplification, although viral RNA was found in low copy number from day 1 p.i. The amplification of negative RNA strand had already been used to evaluate the replication of WNV in spleen by Samuel and Diamond (2005). Similarly, Wang and Deubel (2011) reported low levels of Japanese encephalitis virus (JEV) in spleen of two different murine strains (C3H/HeN and DBA/2) with no signs of viral replication. Similar results were found by Gupta et al. (2010) using JEV in BALB/c mice.

Although SLEV does not replicate in the spleen of the infected mice, we could observe that this tissue is significantly affected after infection. A loss in the follicular architecture was detected in the spleen of mice infected with

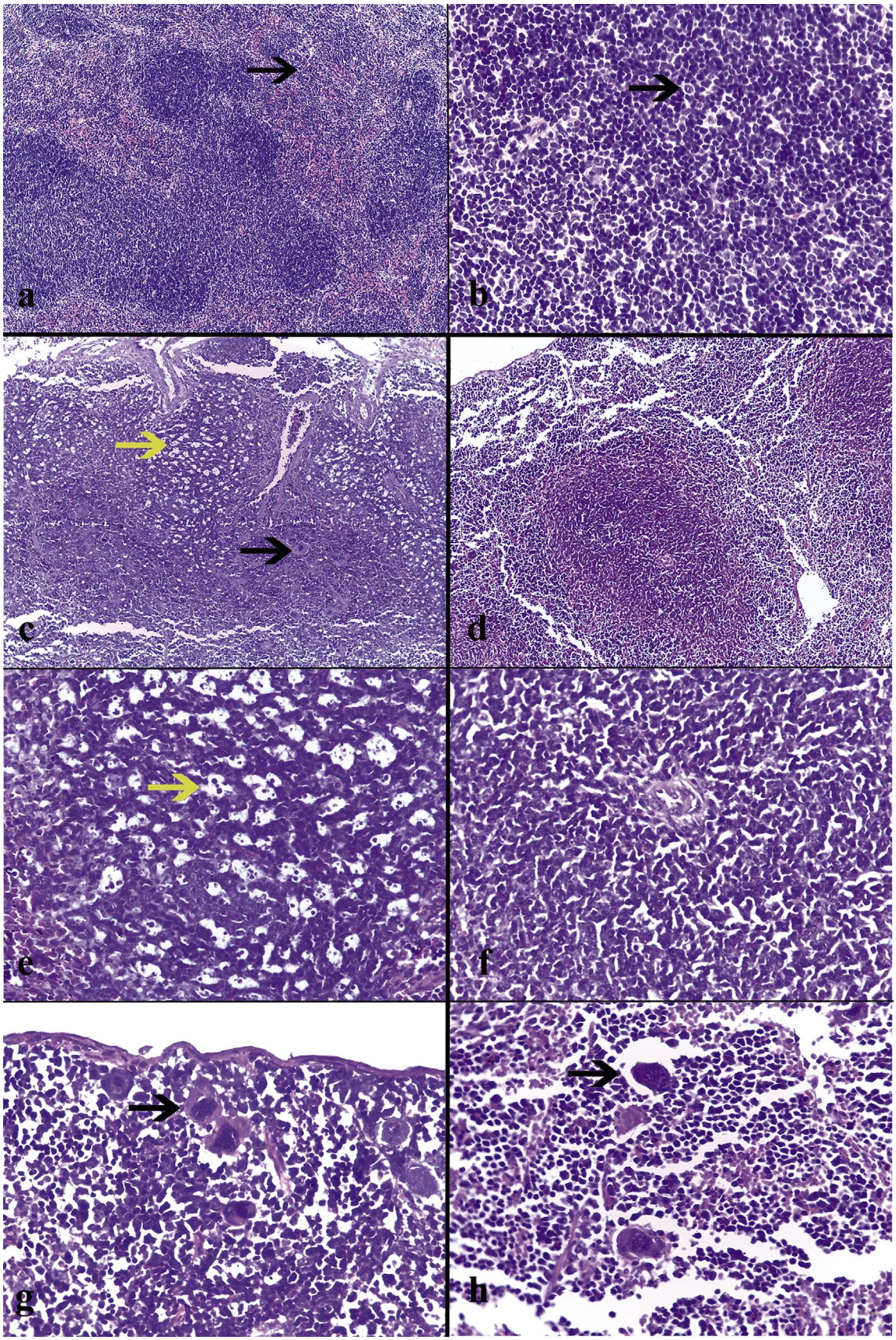

Fig. 4. Histological changes of the spleen of mice infected with CbaAr-4005 and CorAn-9275 strains of SLEV. (a-b) Spleen from uninfected control mouse, HE, 10X and 400X, respectively; the black arrows show megakaryocytes in the perifollicular area. (c-e-g) Spleen from mouse infected with SLEV CbaAr-4005 strain, HE, 10X, 40X and 40X, respectively; the yellow arrows indicate areas typically affected by macrophagy, while the black arrows point at megakaryocytic hiperplasia. (d-f-h) Spleen from mouse infected with SLEV CorAn-9275 strain, HE, 10X, 40X and 40X, respectively. Panel (d) shows follicular hiperplasia in the white pulp; in panel (f) a germinal center is shown with conserved structure; (h) shows the perifollicular region with megakaryocytic hyperplasia (black arrow), HE, 10X. Photographs are representative of one out of 50 mice. (1.5 column-fitting image).

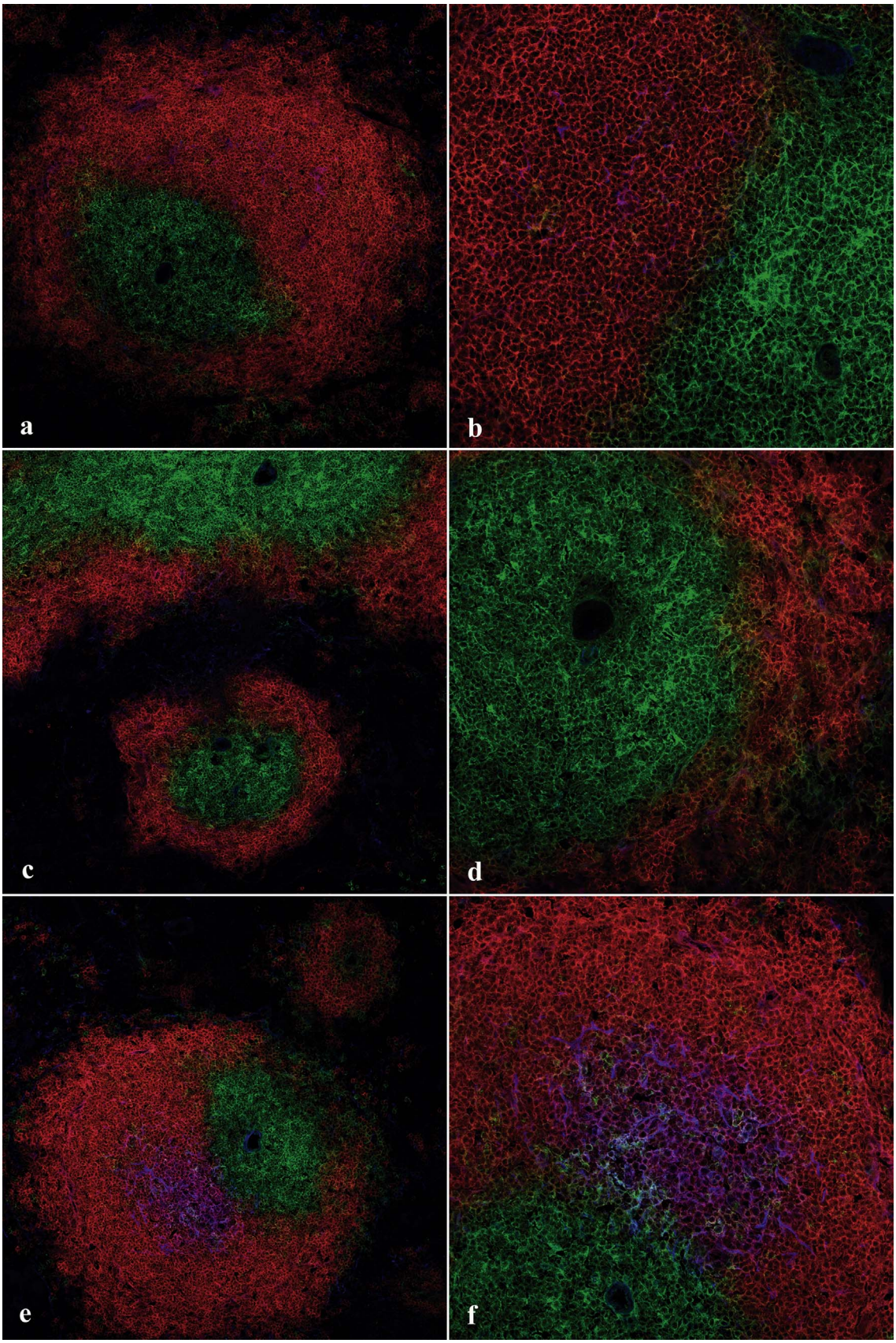

Fig. 5. Lymphocyte distribution in the spleen of mice infected with CbaAr-4005 and CorAn-9275 strains of SLEV. Immunofluorescence of frozen spleen sections (7 μm) from: (a-b) Uninfected control mouse, 20X and 40X, respectively. (*c*-d) mouse infected with SLEV CbaAr-4005 strain, 20X and 40X respectively. (*e*-f) mouse infected with SLEV CorAn-9275 strain, 20X and 40X respectively. The sections were stained with anti-mouse B220 (red), anti-mouse CD4 (green) and PNA (blue) antibodies. The sections shown are representative of four mice at this time point.

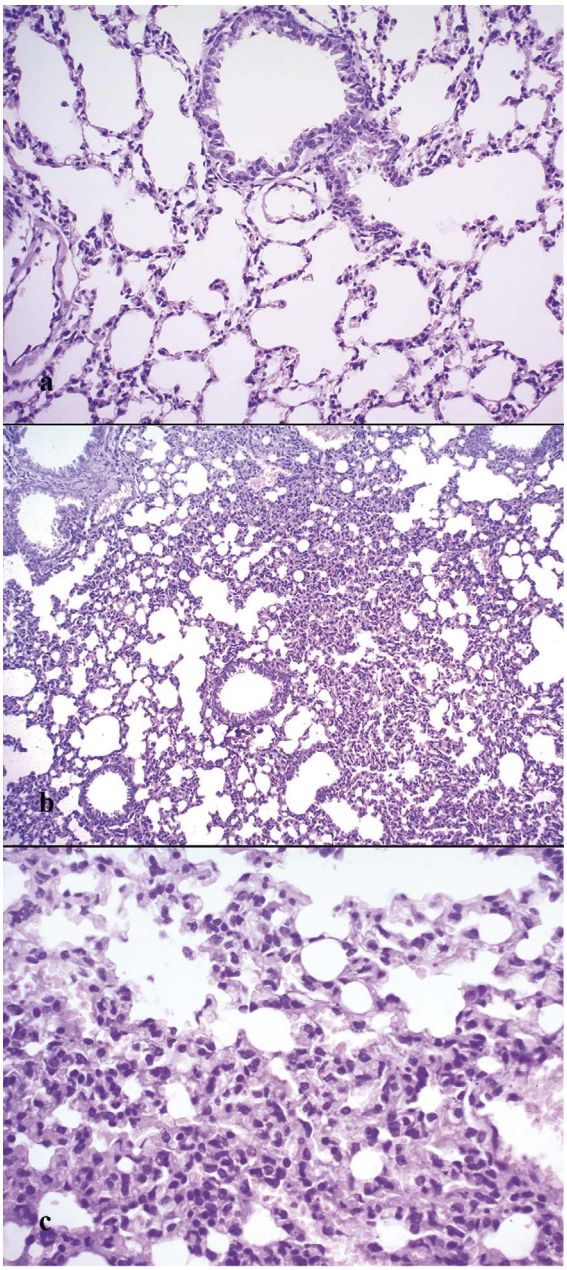

Fig. 6. Lung damage in mouse infected with CbaAr-4005 strain. Photographs of lung sections from (a) control mouse, HE, 20X, and (b-c) CbaAr-4005 infected mouse, HE, 10X and 40X. Panel (b) shows thickened alveolar septa, and (c) shows inflammatory (lymphocytic) infiltrate. Photographs are representative of one out of 50 mice. (Single column-fitting image).

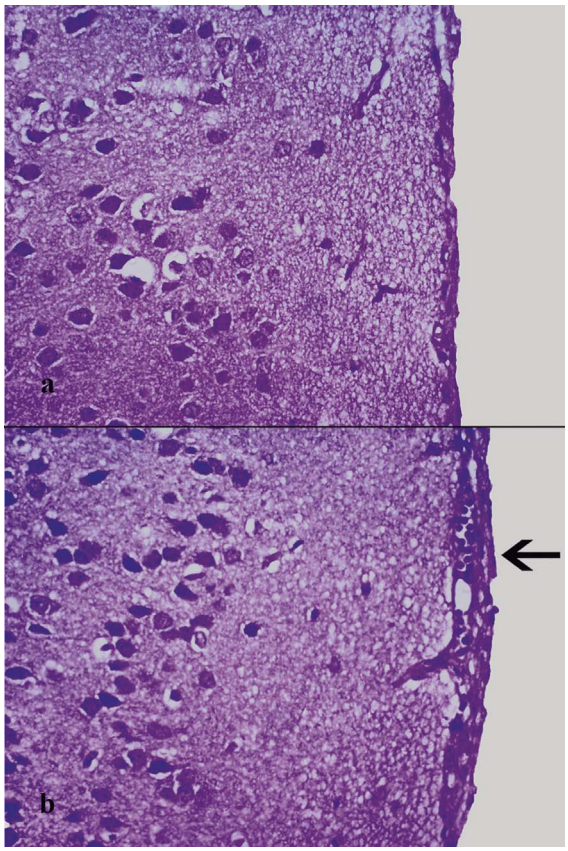

Fig. 7. Development of meningitis after infection with SLEV CbaAr-4005 strain. Photographs of brain sections from (a) uninfected control mouse, HE, 40X, and (b) CbaAr-4005 infected mouse, HE, 40X. The arrow indicates inflamed tissue and the presence of mononuclear lymphocyte-like cells. Photographs are representative of one out of 50 mice. (Single column-fitting image).

CbaAr-4005 strain. These mice had a severe disruption of the splenic white pulp architecture showing, after the infection, scarce B cell follicles and few and irregular GCs, which probably affected the quality of the Ab-secreting cells. This altered morphology could be a consequence of the viral infection and/or destruction of follicular dendritic cells (FDCs), since it has been reported (Wang et al., 2011) that ablation of FDC caused that primary B cell follicles lost their homogeneity and became disorganized, presenting groups of B cells surrounding T cell zones, similar to the belt-like structure we observed after infection with the epidemic SLEV strain. In this sense, Melzi et al. (2016) observed that Bluetongue virus induces an acute immunosuppression by rapidly infecting and destroying FDCs of lymph nodes and hampering the capacity of GCs to produce Abs in sheep. In addition, progressive depletion of proliferating B cells and disruption of the FDC network in GC was evident in the lymph nodes from monkeys collected at 20 days following SIVmac239 challenge (Zhang et al., 2007). Deeper studies should be performed to evaluate the target cells of the CbaAr-4005 virus in the spleen.

In contrast, mice infected with CorAn-9275 strain presented a high number of well-organized GCs, suggesting that they can generate SLEV-specific high affinity Abs to control virus replication. In agreement, mice infected with CorAn-9275 strain, which were able to control the infection, developed neutralizing Abs. Although mice infected with the non-epidemic strain showed neither signs of illness nor mortality, the detection of neutralizing Abs (seroconversion) on day 15 p.i. allows us to confirm that mice were in contact with the virus.

In kidney we detected a low number of copies, with values decreasing towards the end of the experiment. These data differ from results obtained for WNV by Kramer and Bernard (2001) who found that WNV was present in kidney of BALB/c mice by day 2 p.i., with infection levels slowly increasing in this tissue until they reached a peak by day 5 p.i. However, our results indicate that kidney would not be a key target in the tropism of CbaAr-4005 strain. Accordingly, kidneys of mice infected with either CbaAr-4005 or CorAn-9275 strains showed normal histology. Our findings disagree with those informed by Rosa et al. (2013), who reported multifocal hemorrhages and hyperemia in kidneys, brain and lungs.

In lungs, low viral copies were also detected, in agreement with the results documented by Samuel and Diamond (2006), who evaluated viral load values of WNV in C57BL/6 mouse lung. Our histopathological analyses in this organ agree with results of Barth et al. (2006) who reported thickening of alveolar walls and vascular congestion in lungs of BALB/c mice infected with a Brazilian strain of Dengue virus (serotype 2). Rosa et al. (2013) observed strong effects, such as

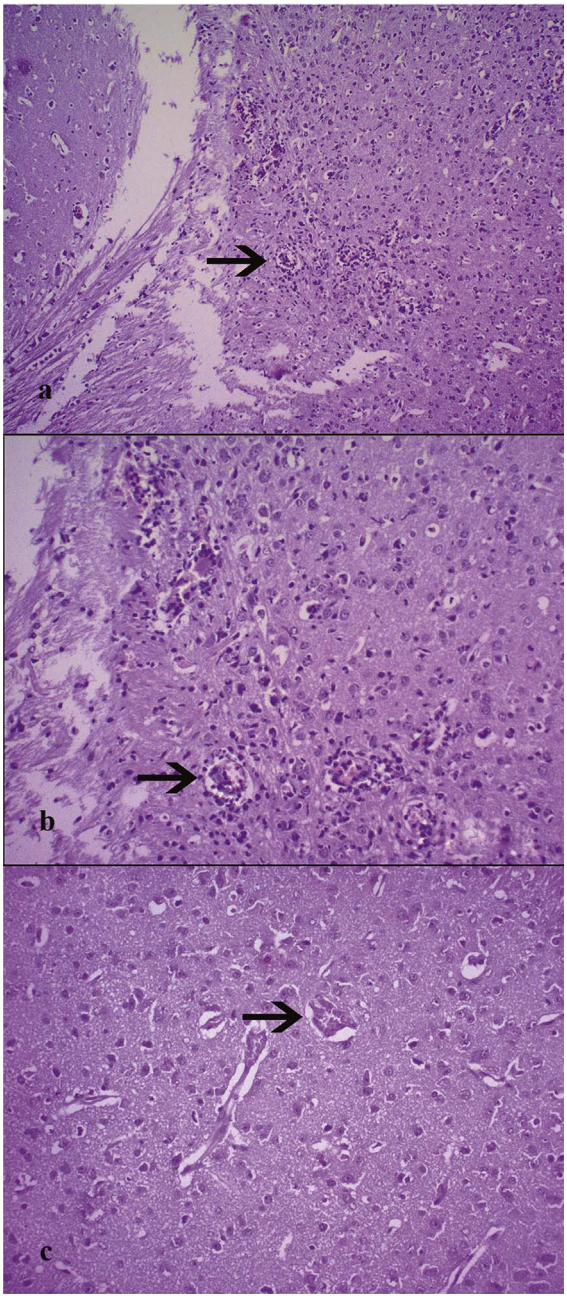

Fig. 8. Inflammatory infiltrate in the brain of mice infected with SLEV CbaAr-4005 strain. Photographs of brain sections from (a-b) brain cortex from infected mouse. Arrows indicate mononuclear lymphocyte-like cells surrounding blood vessels, HE, 20X and 40X respectively. (c) Brain cortex from uninfected mouse. The arrow indicates a blood vessel with no cellular infiltrate, HE, 40X. Photographs are representative of one out of 50 mice. (Single column-fitting image).

hyperemia and multifocal hemorrhages, in lungs of suckling mice infected with a SLEV strain isolated from the brain of a horse with neurological signs from Brazil. Those results may be attributed to the age of mice, since sucklings are more susceptible to infection and to developing strong signs of disease than the 21-day-old animals used in our assays.

Interestingly, our results show that the number of viral RNA copies increases significantly in the brain of infected mice with the epidemic strain. Moreover, replication was also confirmed by negative-strand RT-PCR. Although we did not investigate which is the neuronal type that is specifically targeted by SLEV, experimental evidence with other neurotropic flaviviruses shows that motor neurons and neurons from the limbic system, choroid plexus, and temporal lobe (Whitley and Gnann, 2002) would be typical targets for viral replication. It has been reported that WNV, SLEV and Murray Valley virus activate protective mechanisms in neuronal cells of the cerebellar granular layer and the motor cortex (Omalu et al., 2003; Armah et al., 2007; Cho et al., 2013). It is also well known that some neurotropic viruses can replicate in *in vitro* neuronal cultures. This is the case of WNV, JEV, and SLEV, which replicate in embryonic mouse and rat primary cultures, and in neuroblastoma cells (N2a) (Liao et al., 1997; Heneka and Feinstein, 2001; Parquet et al., 2002). Nevertheless, more studies are needed to elucidate the neuronal target cells and to identify the cerebral areas with neuronal degeneration after infection with the epidemic strain.

CbaAr-4005 was detected in brain until day 8 p.i. The mechanisms that mediate the entry of SLEV into the CNS remain unclear, but it has been shown that the infection of the CNS by WNV is normally associated with a deficient immune response in peripheral tissues where the virus is able to replicate and cause viremia (Cho and Diamond, 2012). Previous studies reported that neuroinvasion of other SLEV strains and WNV occurred in mice at different days p.i. (Monath et al., 1983; Diamond et al., 2003; Wang et al., 2004; Hunsperger and Roehrig, 2006) which may be attributed to differences in viral strain, dose, and route of inoculation. Our results show that all mice exhibited viral particles in the brain on day 5 p.i., simultaneously with the appearance of disease symptoms. Although we cannot correlate the observed symptomatology with affection of specific brain regions, previous reports showed that signs of infection in mice inoculated with SLEV are linked to damages in cerebral cortex and cerebellum (Gardner and Reyes, 1980).

The presence of inflammatory infiltrate in brain is a common fact for many related neurotropic viruses (Smadel and Moore, 1934; Matthews et al., 2000; Shrestha et al., 2003; Shrestha and Diamond, 2004; Gupta et al., 2010;). In our model, the inflammatory infiltrate was detected in the meninges. This finding is consistent with the meningitis reported for mice after infection with other strains of SLEV, WNV and JEV (Wang et al., 2004; Gupta et al., 2010; Rosa et al., 2013). In addition, inflammatory infiltrate showed to be also associated with perivascular spaces, with a higher concentration in the region of the motor cortex. Accordingly, Rosa et al. (2013) detected inflammatory infiltrate confined to the leptomeninges and surrounded by blood vessels in the brain of suckling mice infected with a virulent SLEV strain. They also observed important circulatory changes such as hyperemia and multifocal hemorrhages in brain. The differences with our findings could be due to different factors, such as the use of different viral strains, different ages and degree of development of the immune system in mice, differences in the viral doses used, and strain virulence, among others. Although we did not analyze histopathology using suckling mice, we would expect the same kind of alterations in this age group. In our study, a weak inflammatory process was observed within the brain; this result is consistent with that reported by Monath (1980), who postulated that only minor inflammatory changes can be detected in newborn animals, in which survival times are shorter. These changes can be more developed under conditions of long survival and sublethal encephalitis. Neuronal degeneration has also been reported for other related neurotropic viruses (Bennett et al., 2008; Gupta et al., 2010; Suthar et al., 2010; Lim et al., 2013), and these manifestations are comparable to the ones observed in humans infected with SLEV (Greve et al., 2002).

We demonstrate for the first time the induction of apoptosis in brain by a local epidemic SLEV strain, an effect that has been previously reported in neurons as a consequence of infection by other flavivirus (Hase et al., 1990; Desprès et al., 1998; Shrestha et al., 2003; Samuel et al., 2007). In addition, our group has also proved that this epidemic strain is able to produce apoptosis in infected cultured human monocytes (U937 cells) (personal communication).

Although we detected apoptotic nuclei, we cannot rule out the occurrence of other types of death mechanism, like the ones described

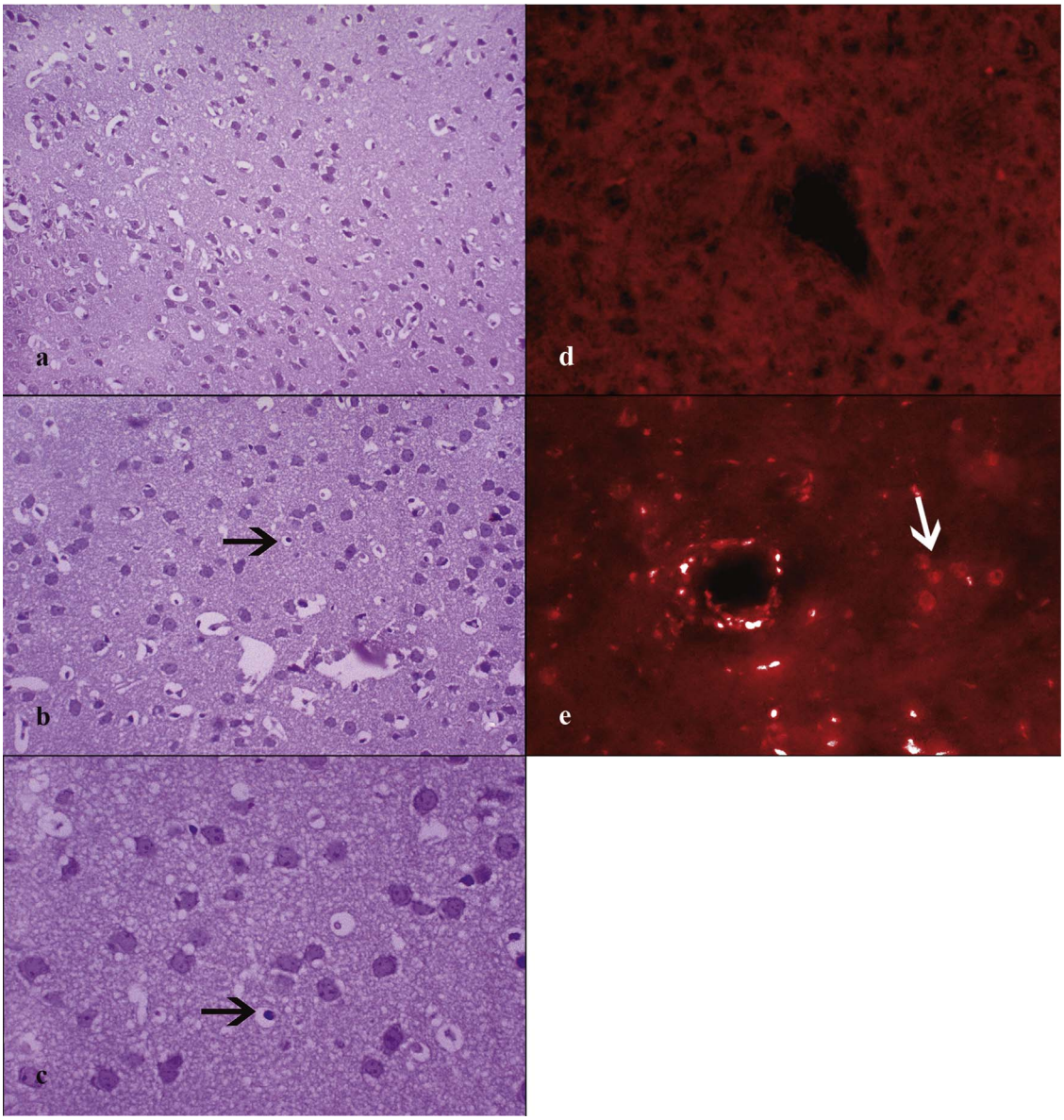

Fig. 9. Cells with apoptotic appearance in brain cortex from mice infected with CbaAr-4005 strain. (*a*-c) Photographs of brain sections stained with HE, showing (a) brain cortex from uninfected mouse, 20X, (b) brain cortex from infected mouse, 20X, and (c) brain cortex from infected mouse, 40X. Black arrows indicate nuclei with apoptotic appearance. Photographs are representative of one out of 50 mice. (*d*-e) Photographs of TUNEL assay showing (d) brain cortex from uninfected mouse, 40X, (e) brain cortex from infected mouse. The white arrow indicates the typical enhanced fluorescence of apoptotic cells, 40X. (1.5 column-fitting image).

by other authors who found necrotic neurons in the brain of mice infected with CHIKV and *Western Equine Encephalitis* virus (WEEV) (Powers and Logue, 2007; Logue et al., 2009).

4. Conclusions

In previous studies carried out in our laboratory, qualitative and quantitative biological markers of virulence were used to compare different local SLEV strains. CbaAr-4005 proved to be more virulent for Swiss albino mice than other non-epidemic variants (Rivarola et al., 2014). Here we show that this virulence can be explained, at least partially, by the capacity of generating high viremia levels, invading and damaging peripheral organs, as well as entering the CNS and causing associated damages. Other aspects, such as the role of the immune response of the host and its contribution to protection or pathology development, will be analyzed in future studies.

5. Materials and methods

5.1. SLEV strains and Mice

Two SLEV strains were used. The endemic strain CorAn-9275 (genotype VII) was isolated from *Mus musculus* in Córdoba province during 1967 (Sabattini et al., 1998). The epidemic strain CbaAr-4005 (genotype III) was isolated from *Culex quinquefasciatus* mosquitoes collected from around the house of SLE-confirmed patients during a human encephalitis outbreak in 2005 in Córdoba (capital city of Córdoba province) (Diaz et al., 2006).

The SLEV stocks used in this study were obtained after five rounds of propagation of the original isolates through suckling mice by means of brain inoculation. Seed stocks for our experiments were prepared by suspending 10% W/V Swiss albino mouse brain in Eagle's minimum essential medium (MEM) supplemented with 10% fetal bovine serum (FBS) and 1% gentamicin. Virus stock titers were determined by standard Vero cell plaque assay and expressed as plaque forming units

per milliliter (PFU/mL) (Contigiani and Sabattini, 1987). Rockefeller Swiss albino mice, strain W1 (R-W1), of 21 days of age were used; all experiments were performed in animal biosafety level 2 facilities. Inbred mice were maintained in the animal house facility of the Arbovirus laboratory of the Virology Institute "Dr. J.M. Vanella" (Universidad Nacional de Córdoba).

5.2. Viremia and survival curves

To analyze the kinetic of viremia, 2 groups of 50 mice were inoculated with 100 µL of viral suspensions containing 3000–5000 PFU/0.1 mL of CbaAr-4005 or CbaAn-9275 strains. Infections were performed by subcutaneous injections to mimic mosquito bites. The control group consisted of 10 mice inoculated with 100 µL of phosphate buffer saline (PBS), instead of viral suspension. Blood samples were taken by cardiac puncture from 5 infected and 1 control mice previously anesthetized with isoflurane during 10 consecutive days after infection. On day 10, mice were euthanized by cervical dislocation. For the viremia analysis, viral loads in blood samples were determined by standard Vero cell plaque assay, and then expressed as logarithm of plaque forming units per milliliter (log PFU/mL) (Contigiani and Sabattini, 1987). Another group of animals was inoculated in parallel, under the same conditions, to analyze subsequent survival. Observations were performed during 15 days p.i. to record any sign of illness (excitability, tremor, laterality on gait and convulsion). Blood samples were collected and sera (1:5 in MEM) were tested for the detection of anti-SLEV neutralizing antibodies (NTAb), using the plaque-reduction neutralization test (Contigiani and Sabattini, 1987).

5.3. In vitro replication curves

A number of 1×10^6 of Vero and Raw 264.7 (murine macrophage) cells/mL, were growth to 90% confluence in 24 plates containing MEM with 10% FCS and 1% gentamicin. Cells were counted by using an automated cell counter (Invitrogen) and infected with CbaAr-4005 and CorAn-9275 strains at m.o.i 1. Infected cells were incubated at 37 °C during 1 h. Virus was removed and monolayers were wash with PBS. MEM 10% FCS and 1% gentamicin was added to each well and cells were incubated al either 37 °C for the duration of experiment. Aliquots of supernatant were removed at 3, 6, 12, 24, 48 and 72 h p.i. and stored at −80 °C for subsequent plaque assay until the monolayers became detached. Virus titration was carried out in duplicate and plaque assay were performed as described (Contigiani and Sabattini, 1987).

5.4. Viral load in tissues

To monitor viral spread after inoculation, kidneys, spleen, lungs, and brain were extracted from the same mice that were sacrificed for viral load determination. A sample of each tissue was weighed and suspended 1/10 W/V in MEM supplemented with 10% FBS and 1% gentamicin. Then, each sample was triturated in a cold mortar, and centrifuged at 9.3*g* for 30 min. Each supernatant was taken for RNA detection and viral load estimation using a quantitative real time PCR (qRT-PCR). Viral loads were expressed in logarithm of copy number per gram. The other samples of each tissue were used for histopathological analyses.

5.5. qRT-PCR

In a first step, RNA from 140 µL of tissue suspension was extracted using AxyPrep viral DNA/RNA MiniPrep kit (CA, USA), following the manufacturer's instructions. For cDNA synthesis, 10 µL of extracted RNA were added to 10 µL of a mixture containing: 1 µL Reverse Transcriptase (ImPromII – Reverse Transcriptase – Promega, Madison WI, USA), 0.5 µL RNase Out (RNase Out Recombinant Ribonuclease Inhibitor, 40 U/µL – Invitrogen, CA, USA), 4 µL buffer 5 (ImPromII – Reverse Transcriptase – Promega, Madison WI, USA), 2.4 µL MgCl2 25 mM, 1 µL random primers (10 pmol/µL) (Promega, Madison WI, USA), 1 µL dNTPs (10 mM each dATP, dCTP, dGTP, and dTTP), and 0.1 µL free RNase water (final volume: 20 µL).

In order to quantify the viral copies in the selected organs, a qRT-PCR was developed. A multiple alignment was carried out using the Clustal W program with complete genome sequences from several Flavivirus species (Dengue, Japanese encephalitis, Murray Valley, Rocio, SLEV, Usutu, West Nile and Yellow Fever and viruses), obtained from GenBank (National Center for Biotechnology Information). Specific primers and TaqMan-MGB fluorescent probes were designed manually within the 3´non-coding region of the flavivirus genome for use in qRT-PCR, which were evaluated with the primer probe test tool of Primer Express® software (version 2.0.0) (Applied Biosystems). Moreover, an internal amplification control (IAC) was developed and included in the reaction in order to prevent false negative results that might be caused by PCR inhibitors. For this purpose, an IC DNA fragment was obtained by an overlap extension PCR carried out using IC-F (5´-GAGGTTAGAGGAGACCCCGCCCAGCACACATGTGTCTACT-3´) and IC-Re (5´-GTCTCCTCTAACCTCTAGTCCTTCCCAGTAGACAC ATGTGTGCTGG-3´) primers. The product was cloned and sequenced, and the cloned DNA contained the binding sites for the SLEV-F and SLEV-Re primers, flanking the heterologous sequence selected as the IC probe. The qRT-PCR assay was developed using a unique pair of competitive primers and two specific TaqMan-MGB fluorescent probes, labeled at the 5´end with VIC for SLEV and NED for internal control (IC) (Table 1).

The reproducibility and stability of the assay was determined. Each dilution was extracted and amplified three times in the same run to evaluate intra-experimental reproducibility and in three different runs to evaluate inter assay variation.

The TaqMan qRT-PCR assays were performed in a final volume of 30 µL. Briefly, 5 µL of cDNA were added to 25 µL of a PCR mix containing 12.5 µL of buffer 2X (Applied Biosystem), 0.2 µL of primer SLEV+1 (100 µM), 0.3 µL of primer SLEV-1 (100 µM), 1 µL of TaqMan VIC labeled probe (5 µM), 1 µL of TaqMan NED labeled probe (5 µM), 0.5 µL of IC (1000 copies) and 9.5 µL of RNAse free water. Samples underwent an initial denaturation and activation phase for polymerase at 95 °C for 15 min, followed by further 40 cycles of 95 °C for 15 s and 60 °C for 1 min. Assays were run in an Applied Biosystems 7500 equipment. Viral copies were estimated by interpolation with a standard curve obtained by serial dilutions of a control plasmid (10 to10^9 copy number).

Table 1
Primers and probes used in the TaqMan qRT-PCR designed for SLEV.

Name	Sequence and labeling	Genome position
Primers		
SLEV-F	5′-GAGGTTAGAGGAGACCCCGC-3′	10717–10736
SLEV-Re	5′-GTCTCCTCTAACCTCTAGTCCTTCCC-3	10781–10806
Probes		
SLEV_Probe	5′-VIC-AACTTGGCAAGGCC-3′-MGB	10740–10753
CI_ProbeSLEV_Probe	5´-NED- CCAGCACACATGTGTCTA-3´-MGB	
CI_Probe	5′-VIC-AACTTGGCAAGGCC-3′-MGB	10740–10753
	5´-NED- CCAGCACACATGTGTCTA-3´-MGB	

*Genome position refers to SLEV complete genome strain 79V-2533 (GenBank accession number FJ753287). F: sense orientation. Re: antisense orientation.

5.6. Strand-specific RT-PCR

To directly evidence viral replication in the analyzed organs of mice infected with SLEV CbAr-4005, a negative-strand-specific RT-PCR was performed. Complementary DNA was synthesized as follows: 10 μL of extracted RNA were added to 10 μL of a mixture containing 1 μL Reverse Transcriptase (ImPromII – Reverse Transcriptase – Promega, Madison WI, USA), 0.5 μL RNase Out (RNase Out Recombinant Ribonuclease Inhibitor, 40 U/μL – Invitrogen, CA, USA), 4 μL buffer 5 (ImPromII – Reverse Transcriptase – Promega, Madison WI, USA), 2.4 μL MgCl2 25 mM, 1 μL (10 pmol) of the positive strand primer SLE2002 (Ré et al., 2008), 1 μL dNTPs (10 mM each dATP, dCTP, dGTP, and dTTP), and 0.1 μL free RNase water (final volume: 20 μL) The amplification of the negative strand of a fragment including parts of NS1 and E proteins of SLEV was performed in two steps following the procedure detailed in Ré et al. (2008). PCR products were subjected to agarose gel electrophoresis for the visualization of bands.

5.7. Histopathological assays

Organs were collected at day 7 p.i. and approximately 50% of each tissue sample, including kidneys, spleen, lungs and brain, was fixed overnight in 10% buffered formalin (BF) and then sectioned in paraffin. For histological examination, sagittal sections of the tissues (4 μm) were stained with hematoxylin and eosin (HE) (Daffis et al., 2008; Logue et al., 2009). Micrographs were taken using an AxioCam Erc DPX camera attached to an Olympus CX40 microscope.

5.8. Immunofluorescence

For tissue immunofluorescence, spleens from control and infected mice were collected and frozen over liquid nitrogen. Frozen sections 7 μm in thickness were cut, fixed for 10 min in cold acetone, left to dry at 25 °C and stored at −80 °C until use. Slides were hydrated in TRIS buffer and blocked for 30 min at 25 °C with 10% normal mouse serum in TRIS buffer. After blockade, slides were incubated for 60 min at 25 °C with a "cocktail" containing Alexa Fluor 488-labeled anti CD4, PE-labeled anti. B220 and Alexa Fluor 647-labeled PNA diluted in TRIS Buffer. Slices were mounted with FluorSave (Merck Millipore). Images were collected with an Olympus microscope (FV1000) and those recorded in the far-red channel were pseudocolored blue.

5.9. In situ TUNEL assay

A group of brains obtained from CbaAr-4005 and control infected mice were cut at 25 μm in a cryostat (Leica Biosystems, Germany) and directly mounted on gelatine coated slides for apoptosis evaluation by the TUNEL (terminal deoxynucleotidyltransferase-mediated dUTP-biotin nick end labeling, Roche) technique.

A series of sagittal sections were hydrated in PBS for 30 min. Then a permeabilizing solution containing 0.1% Triton in 0.1% sodium citrate was added, and the sections where incubated for 2 min. After 3 washes with PBS, a 20 μL of TUNEL mix containing 50 μL of terminal deoxynucleotidyl transferase (TdT) enzyme in 450 μL of dye solution was added. A 20 μL dye solution was used as negative control. The sections were then incubated in darkness in humid chamber at 37 °C. Finally the sections where washed 3 times in PBS and mounted with Fluor-Save (Sigma). Micrographs were taken using an inverted fluorescence microscope (Olympus IX81, Imaging Software: Cell M) with rhodamine filter (653 nm).

5.10. Statistical analyses

The significance and magnitude of the variation of viral tropism within and between organs and dpi was explored. Generalized least squares modeling (GLS) was chosen for estimating the unknown parameters and to model the heterogeneity of residuals using the package “nlme” (Pinheiro et al., 2016). A logarithmic transformation of the copy numbers obtained by qRT-PCR was used to deal with the skewed nature of the dataset. Multiple comparison procedures were chosen for estimating the possible contrasts with Tukey's test and Bonferroni correction, using the “multcomp” (Hothorn et al., 2008) and the “factorplot” (Armstrong, 2016) packages. The graphical explorations of data were perfomed with “ggplot2″ (Wickham, 2009) and “sciplot” (Morales and R Development Core Team, 2012). All the mentioned packages and statistical analyses were implemented in R (R Development Core Team, 2008).

5.11. Ethics statement

All procedures followed the guidelines of the Institutional Committee for the Care and Use of Laboratory Animals from the School of Medicine of the National University of Córdoba, in accordance with the NIH-USA (1996) Guidelines for the Care and Use of Laboratory Animals and the EC Directive 86/609. The Institutional Committee approved the experimental procedures involving animals described in our study (Identification number: 02/13–674/09).

Acknowledgements

We thank Martín López and Fernando Farías for technical assistance in the maintenance of mice facility, Dr. Hugo Cejas for his contributions to the histological analyses of tissues, Dr. Soledad de Olmos for her contributions to histological assays, and Virored-Cyted.

This study was supported by funding from the Fondo Nacional para la Investigación Científica y Tecnológica (FONCyT, PICT 2013 N°1779), Fundación Alberto J. Roemmers (2013–2015) and MINCyT Cba. PID. RES: 000113/2011. Dr. Rivarola and Dr. Gorosito-Serrán are postdoctoral fellows of CONICET. Cristian G. Beccaria is a doctoral fellow of CONICET. Drs. Gruppi, Albrieu-Llinás, Pisano, Tauro, and Díaz are researchers of CONICET.

References

Armah, H.B., Wang, G., Omalu, B.I., Tesh, R.B., Gyure, K.A., Chute, D.J., Wiley, C.A., 2007. Systemic distribution of West Nile virus infection: postmortem immunohistochemical study of six cases. Brain Pathol. 17, 354–362.

Armstrong, D. factorplot: Graphical Presentation of Simple Contrasts. R package version 1.1-2. "⟨https://cran.r-project.org/web/packages/factorplot/index.html⟩ (last accessed 30.09.16).

Arroyo, J., Guirakhoo, F., Fenner, S., Zhang, Z.X., Monath, T.P., Chambers, T.J., 2001. Molecular basis for attenuation of neurovirulence of a yellow fever Virus/Japanese encephalitis virus chimera vaccine (ChimeriVax-JE). J. Virol. 75, 934–942.

Barth, O.M., Barreto, D.F., Paes, M.V., Takiya, C.M., Pinhão, A.T., Schatzmayr, H.,G., 2006. Morphological studies in a model for dengue-2 virus infection in mice. Mem. do Inst. Oswaldo Cruz 101, 905–915.

Beasley, D.W., Davis, C.T., Whiteman, M., Kinney, R.M., Barrett, A.D., 2004. Molecular determinants of virulence of West Nile virus in North America. In: Calisher, C.H., Griffin, D.E., Wien (Eds.), Emergence and Control of ZoonoticViral Encephalitides. A: Springer-Verlag Press, 35–41.

Ben-Nathan, D., Huitinga, I., Lustig, S., Kobiler, D., 1996. West Nile virus neuroinvasion and encephalitis induced by macrophages depletion in mice. Arch. Virol. 141, 459–469.

Bennett, R.S., Cress, C.M., Ward, J.M., Firestone, C.Y., Murphy, B.R., Whitehead, S.S., 2008. La Crosse virus infectivity, pathogenesis, and immunogenicity in mice and monkeys. J. Virol. 5, 25, (doi:10 1186/1743-422X-5-25).

Bowen, G.S., Monath, T.P., Kemp, G.E., Kerschner, J.H., Kirk, L.J., 1980. Geographic variation among St. Louis encephalitis virus strains in the viremic responses of avian hosts. Am. J. Trop. Med. Hyg. 29, 1411–1419.

Brown, A., Kent, K., Bennett, J.C., Bernard, K., 2007. Tissue tropism and neuroinvasion of West Nile virus do not differ for two mouse strains with different survival rates. Virology 368, 422–430.

Calisher, C.H., 1994. Medically important arboviruses of the United States and Canada. Clin. Microbiol. 7, 89–116.

Cho, H., Diamond, M.S., 2012. Immune Responses to West Nile Virus Infection in the Central Nervous System. Viruses 4 (12), 3812–3830.

Cho, H., Proll, S.C., Szretter, K.J., Katze, M.G., Gale, M., Jr., Diamond, M.S., 2013. Differential innate immune response programs in neuronal subtypes determine susceptibility to infection in the brain by positive stranded RNA viruses. Nat. Med. 19 (4), 458–464.

Contigiani, M.S., Sabattini, M.S., 1987. Heterogeneity in the virulence of viral subpopulations derived from an attenuated strain of Junin virus. Rev. Latinoam. De. Microbiol. 29, 345–352.
Daffis, S., Samuel, M.A., Suthar, M.S., Keller, B.C., Gale, M., Jr., Diamond, M.S., 2008. Interferon regulatory factor IRF-7 induces the antiviral alpha interferón response and protects against lethal West Nile virus infection. J. Virol. 82, 8465–8475.
Desprès, P., Pascalefrenkiel, M., Ceccaldi, P.E., Duarte Dos Santos, C., Deubel, V., 1998. Apoptosis in the mouse central nervous System in response to infection with mouse-neurovirulent dengue viruses. J. Virol. 72 (1), 823–829.
Diamond, M.S., Shrestha, B., Marri, A., Mahan, D., Engle, M., 2003. B Cells and Antibody Play Critical Roles in the Immediate Defense of Disseminated Infection by West Nile Encephalitis Virus. J. Virol. 77, 2578–2586.
Diaz, L.A., Goñi, S.E., Iserte, J.A., Quaglia, A.I., Singh, A., Logue, C.H., Powers, A.M., Contigiani, M.S., 2015. Exploring Genomic, Geographic and Virulence Interactions among Epidemic and Non-Epidemic St. Louis encephalitis virus (Flavivirus) Strains. Plos One 10 (8), e0136316. http://dx.doi.org/10.1371/journal.pone.0136316.
Diaz, L.A., Ré, V., Almirón, W.R., Farías, A., Vásquez, A., Sanchez Seco, M.P., Aguilar, J., Spinsanti, L., Konigheim, B., Visintin, A., et al., 2006. Genotype III Saint Louis encephalitis virus Outbreak, Argentina, 2005. Emergin Infect. Dis. 12 (11), 1752.
Gardner, J.J., Reyes, M.G., 1980. Pathology. (American Public Health Association)In: Monath, T.P. (Ed.), St. Louis encephalitis. CRC Press, Washington, DC, 551–569.
Greve, K.W., Houston, R.J., Adams, D., Stanford, M.S., Bianchini, K.J., Clancy, A., Rabito, F.J., 2002. The neurobehavioural consequences of St. Louis encephalitis infection. Brain Inj. 16, 917–927.
Griffin, D.E., Levine, B., Tucker, P.C., Hardwick, J.M., 1994. Age-dependent susceptibility to fatal encephalitis: alphavirus infection of neurons. Arch. Virol. 9, 31–39.
Gupta, N., Lomashb, V., Lakshmana Raoa, P.V., 2010. Expression profile of Japanese encephalitis virus induced neuroinflammation and its implication in disease severity. J. Clin. Virol. 49, 4–10.
Hase, T., Summers, P.L., Dubois, D.R., 1990. Ultrastructural changes of mouse brain neurons infected with Japanese encephalitis virus. Int. J. Exp. Pathol. 71, 493–505.
Heneka, M.T., Feinstein, D.L., 2001. Expression and function of inducible nitric oxide synthase in neurons. J. Neuroimmunol. 114, 8–18.
Hothorn, T., Frank Bretz, F., Westfall, P., 2008. Simultaneous Inference in General Parametric Models. Biom. J. 50 (3), 346–363.
Hunsperger, E.A., Roehrig, J.T., 2006. Temporal analyses of the neuropathogenesis of a West Nile virus infection in mice. J. Neurovirol. 12, 129–139.
King, N.J.C., Getts, D.R., Getts, M.T., Rana, S., Shrestha, B., Kesson, A.M., 2007. Immunopathology of flavivirus infection. Immunol. Cell Biol. 85, 33–42.
Kramer, L.D., Chandler, L.J., 2001. Phylogenetic analysis of the envelope gene of St. Louis encephalitis virus. Arch. Virol. 146 (12), 2341–2355.
Kramer, L.D., Bernard, K.A., 2001. West Nile virus infection in birds and mammals. Ann. New Y. Acad. Sci. 951, 84–93.
Liao, C.L., Lin, Y.L., Wang, J.J., Huang, Y.L., Yeh, C.T., Ma, S.H., Chen, L.K., 1997. Effect of enforced expression of human Bcl-2 on Japanese encephalitis virus-induced apoptosis in cultured cells. J. Virol. 71, 5963–5971.
Lim, S.M., Koraka, P., van Boheemen, S., Roose, J.M., Jaarsma, D., van de Vijver, D.A., Osterhaus, A.D.M.E., Martina, B.E.E., 2013. Characterization of the mouse neuroinvasiveness of selected European strains of West Nile virus. PloS One 8 (9), e74575.
Logue, C.H., Bosio, C.F., Welte, T., Keene, K.M., Ledermann, J.P., Philips, A., Sheahan, B.J., Pierro, D.J., Marlenee, N., et al., 2009. Virulence variation among isolates of western equine encephalitis virus in an outbred mouse model. J. Gen. Virol. 90, 1848–1858.
Mandl, C.W., Allison, S.L., Holzmann, H., Meixner, T., Heinz, F.X., 2000. Attenuation of tick-borne encephalitis virus by structure-based site-specific mutagenesis of a putative flavivirus receptor binding site. J. Virol. 74, 9601–9609.
Matthews, V., Robertson, T., Kendrick, T., Abdo, M., Papadimitriou, J., McMinn, P., 2000. Morphological features of Murray Valley encephalitis virus infection in the central nervous system of swiss mice. Int. J. Exp. Pathol. 81, 31–40.
McMinn, P.C., 1997. The molecular basis of virulence of the encephalitogenic flaviviruses. J. Gen. Virol. 78, 2711–2722.
Mehlhop, E., Diamond, M.S., 2007. Complement protein C1q inhibits antibody-dependent enhancement of flavivirus infection in an IgG subclass-specific manner. Cell Host Microbe 2, 417–426.
Melzi, E., Caporale, M., Rocchi, M., Martin, V., Gamino, V., di Provvido, A., Marruchella, G., Entrican, G., Sevilla, N., Palmarini, M., 2016. Follicular dendritic cell disruption as a novel mechanism of virus-induced immunosuppression. PNAS, E6238–E6247.
Monath, T.P., 1980. Epidemiology. In: Monath, T.P. (Ed.), St. Louis Encephalitis. American Public Health Association, Washington, DC, 239–312.
Monath, T.P., Borden, E., 1971. Effects of thorotrast on humoral antibody, viral multiplication, and interferon during infection with St. Louis encephalitis virus in mice. J. Infected Dis. 123, 297–300.
Monath, T.P., Cropp, C.B., Harrison, A.K., 1983. Mode of entry of a neurotropic arbovirus into the central nervous system. Reinvestigation of an old controversy. Lab. Investig. J. Tech. Methods Pathol. 48 (4), 399–410.
Monath, T.P., Cropp, C.B., Bowen, G.S., Kemp, G.E., Mitchell, C.J., Gardner, J.,J., 1980. Variation in virulence for mice and rhesus monkeys among St. Louis encephalitis virus strains of different origin. Am. J. Trop. Med. Hyg. 29, 948–962.
Mondini, A., Bronzoni, R.V., Cardeal, I.L., dos Santos, T.M., Lázaro, E., Nunes, S.H., Dutra Silva, G.C., Ferrari Sarkis Madris, M.C., Rahal, P., Figueiredo, L.T., et al., 2007. Simultaneous infection by DENV-3 and SLEV in Brazil. J. Clin. Virol. 40 (1), 84–86.
Morales, M., R Development Core Team. Sciplot: Scientific Graphing Functions for Factorial Designs. ⟨https://cran.r-project.org/web/packages/sciplot/index.html⟩ (last accessed 30.09.12).
Muylaert, I.R., Chambers, T.J., Galler, R., Rice, C.M., 1996. Mutagenesis of the N-linked glycosylation sites of the yellow fever virus NS1 protein: effects on virus replication and mouse neurovirulence. Virology 222, 159–168.
Omalu, B.I., Shakir, A.A., Wang, G., Lipkin, W.I., Wiley, C.A., 2003. Fatal fulminant pan-meningopolioencephalitis due to West Nile virus. Brain Pathol. 13, 465–472.
Ong, R.Y., Lum, F.M., Lisa, F.P., Ng, L.F.P., 2014. The fine line between protection and pathology in neurotropic flavivirus and alphavirus infections. Future Virol. 9 (3), 313–330.
Parquet, M.C., Kumatori, A.K., Mathenge, E.G.M., Mathenge, E.G., Morita, K., 2002. St. Louis encephalitis virus induced pathology in cultured cells. Arch. Virol. 147, 1105–1119.
Pinheiro, J., Bates, D., DebRoy, S., Sarkar, D., Core Team, R.. nlme: Linear and Nonlinear Mixed Effects Models. R package version 3.1-128. ⟨http://CRAN.R-project.org/package=nlme⟩ (last accessed 30.09.16).
Pletnev, A.G., Bray, M., Lai, C.J., 1993. Chimeric tick-borne encephalitis and dengue type 4 viruses: effects of mutations on neurovirulence in mice. J. Virol. 67, 4956–4963.
Powell, K.E., Kappus, K.D., 1978. Epidemiology of St. Louis encephalitis and other acute encephalitides. Advaces Neurol. 19, 197–213.
Powers, A.M., Logue, C.H., 2007. Changing patterns of chikungunya virus: re-emergence of a zoonotic arbovirus. J. Gen. Virol. 88, 2363–2377.
R Development Core Team, 2008. R: a language and environment for statistical computing. R Foundation for Statistical Computing, Vienna, Austria, (ISBN 3-900051-07-0, URL)⟨http://www.R-project.org⟩.
Ré, V., Spinsanti, L., Farías, A., Vázquez, A., Aguilar, J., Tenorio, A., Contigiani, M., 2008. Reliable detection of St. Louis encephalitis virus by RT-nested PCR. Enferm. Infecc. Y. Microbiol. Clin. 26 (1), 10–15.
Reisen, W.K., 2003. Epidemiology of St. Louis Encephalitis virus. Adv. Virus Res. 61, 139–183.
Rivarola, M.E., Tauro, L.B., Albrieu-Llinás, G., Contigiani, M.S., 2014. Virulence variation among epidemic and non-epidemic strains of Saint Louis encephalitis virus circulating in Argentina. Mem. do Inst. Oswaldo Cruz 109 (2), 197–201.
Rocco, I.M., Santos, C.L., Bisordi, I., Petrella, S.M., Pereira, L.E., Souza, R.P., Coimbra, T.L.M., Bessa, T.A.F., Oshiro, F.M., Lima, L.B.Q., et al., 2005. St. Louis encephalitis virus: first isolation from a human in São Paulo state, Brazil. Rev. do Inst. Med. Trop. De. Sao Paulo 47 (5), 281, (-5.3).
Rodrigues, S.G., Nunes, M.R., Casseb, S.M., Prazeres, A.S., Rodrigues, D.S., Silva, M.O., Cruz, A.C.R., Tavares-Neto, J.C., Vasconcelos, P.F.C., 2010. Molecular epidemiology of Saint Luois encephalitis virus in the Brazilian Amazon: genetic divergence and dispersal. J. Gen. Virol. 91, 2420–2427.
Rosa, R., Azevedo Costa, E., Marquez, R.E., Oliveira, T.S., Furtini, R., Quaresma Bomfin, M.R., Teixeira, M.M., Paixao, T.A., Lima Santos, R., 2013. Isolation of Saint Louis encephalits virus from a horse with neurological disease in Brazil. PLoS Negl. Trop. Dis. 7 (11), e2537. http://dx.doi.org/10.1371/journal.pntd.0002537.
Sabattini, M.S., Avilés, G., Monath, T.P., 1998. Historical epidemiological and ecological aspects of arbovirus in Argentina: flaviviridae, Bunyaviridae and Rhadboviridae. In: Travassos da Rosa, A.P.A., Vasconcelos PFC, P.F.C., Travassos da Rosa JFS, J.F.S. (Eds.), An overview of arbovirology in Brazil and neighbouring countries. Instituto Evandro Chagas, Be: Brazil, 135–153.
Samuel, M.A., Diamond, M.S., 2005. Alpha/Beta Interferon Protects against Lethal West Nile Virus Infection by Restricting Cellular Tropism and Enhancing Neuronal Survival. J. Virol. 79, 13350–13361.
Samuel, M.A., Diamond, M.S., 2006. Pathogenesis of West Nile Virus Infection: a balance between virulence, innate and adaptive immunity and viral evasion. Jounal Virol. 80, 9349–9360.
Samuel, M.A., Morrey, J.D., Diamond, M.S., 2007. Caspase 3-dependent cell death of neurons contributes to the pathogenesis of West Nile virus encephalitis. J. Virol. 81, 2614–2623.
Seijo, A., Morales, A., Poustis, G., Romero, Y., Efron, E., Vilora, G., Lloveras, S., Giamperetti, S., Monroig, J., Luppo, V., Enría, D., 2011. Outbreak of St. Louis encephalitis in the metropolitan Buenos Aires area. Med. (B Aires) 71, 211–217.
Shrestha, B., Diamond, M.S., 2004. Role of CD8_ T Cells in Control of West Nile Virus Infection. J. Virol. 78, 8312–8321.
Shrestha, B., Gottlieb, D., Diamond, M.S., 2003. Infection and Injury of Neurons by West Nile Encephalitis Virus. J. Virol. 77, 13203–13213.
Smadel, J.F., Moore, E., 1934. Changes produced in the central nervous system of the mouse by the virus St. Louis encephalitis. Am. J. Pathol. 10, 827.
Solomon, T., Vaughn, D.W., 2002. Pathogenesis and clinical features of Japanese encephalitis and West Nile virus infections. Curr. Top. Microbiol. Immunol. 267, 171–194.
Spinsanti, L., Basquiera, A., Bulacio, S., Somale, V., Kim, S.C.H., Ré, V., Rabbat, D., Zárate, A., Zlocowski, J.C., Quiroga Mayor, C., et al., 2003. St. Louis encephalitis in Argentina: the first case reported in the last seventeen years. Emerg. Infect. Dis. 9, 271–273.
Spinsanti, L.I., Díaz, L.A., Glatstein, N., Arzelán, S., Morales, M.A., Farías, A.A., Fabbri, C., Aguilar, J.J., Ré, V., Frías, M., et al., 2008. Human outbreak of St. Louis encephalitis detected in Argentina, 2005. J. Clin. Virol. 42, 27–33.
Steele, K.E., Twenhafel, N.A., 2010. Pathology of animal models of alphavirus encephalitis. Vet. Pathol. 47 (5), 790–805.
Suthar, M.S., Ma, D.Y., Thomas, S., Lund, J.M., Zhang, N., Daffis, S., Rudensky, A., Bevan, M.J., Clark, E.A., Kaja, M.K., et al., 2010. IPS-1 is essential for the control of West Nile virus infection and immunity. PLoS Pathog. 6 (2), e1000757.
Trent, D.W., Monath, T.P., Bowen, G.S., Vorndam, A.V., Cropp, C.B., Kemp, G.E., 1980. Variation among strains of St. Louis encephalitis virus: basis for a genetic, pathogenic and epidemiological classification. Ann. New Y. Acad. Sci. 354, 219–237.
Vogel, P., Kell, W.M., Fritz, D.L., Parker, M.D., Schoepp, R.J., 2005. Early Events in the

Pathogenesis of Eastern Equine Encephalitis Virus in Mice. Am. J. Pathol. 166 (1), 159–171.

Wang, K., Deubel, V., 2011. Mice with Different Susceptibility to Japanese Encephalitis Virus Infection Show Selective Neutralizing Antibody Response and Myeloid Cell Infectivity. PLoS One 6, e24744. http://dx.doi.org/10.1371/journal.pone.0024744.

Wang, T., Town, T., Alexopoulou, L., Anderson, J.F., Fikrig, E., Flavell, R.A., 2004. Toll-like receptor 3 mediates West Nile virus entry into the brain causing lethal encephalitis. Nat. Med. 10, 1366–1373.

Wang, X., Cho, B., Zuzuki, K., Xu, Y., Green, J.A., An, J., Cyster, J.G., 2011. Follicular dendritic cells help establish follicle identity and promote B cell retention in germinal centers. J. Exp. Med. 12, 2497–2510.

Wang, Y., Lobigs, M., Lee, E., Mullbacher, A., 2003. CD8-T Cells Mediate Recovery and Immunopathology in West Nile Virus Encephalitis. J. Virol. 77, 13323–13334.

Weiner, L.P., Cole, G.A., Nathanson, Neal, 1970. Experimental encephalitis following peripheral inoculation of West Nile virus in mice of different ages. J. Hyg. 68 (3), 435–446.

Whitley, R.J., Gnann, J.W., 2002. Viral encephalitis: familiar infections and emerging pathogens. Lancet 359, 507–513.

Wickham, H., 2009. ggplot2: elegant Graphics for Data Analysis. Springer-Verlag, New York.

Zhang, Z.Q., Casimiro, D.R., Schleif, W.A., Chen, M., Citron, M., Davies, M.E., Burns, J., Xiaoping Liang, X., et al., 2007. Early depletion of proliferating B cells of germinal center in rapidly progressive simian immunodeficiency virus infection. Virology 10 (2), 455–464.